

OPTICAL COHERENCE TOMOGRAPHY

PACS numbers: 42.30.Wb; 87.19.xj; 87.63.lt
DOI: 10.1070/QE2014v044n12ABEH015380

Monitoring of permeability of different analytes in human normal and cancerous bladder tissues *in vitro* using optical coherence tomography

Bingsong Lei, Xiaoyuan Deng, Huajiang Wei, Guoyong Wu, Zhouyi Guo, Hongqin Yang, Yonghong He, Shusen Xie

Abstract. **We report our preliminary results on quantification of glucose and dimethyl sulfoxide (DMSO) diffusion in normal and cancerous human bladder tissues *in vitro* by using a spectral domain optical coherence tomography (SD-OCT). The permeability coefficients (PCs) of a 30% aqueous solution of glucose are found to be $(7.92\pm0.81)\times10^{-6}$ cm s^{-1} and $(1.19\pm0.13)\times10^{-5}$ cm s^{-1} in normal and cancerous bladder tissues, respectively. The PCs of 50% DMSO are calculated to be $(8.99\pm0.93)\times10^{-6}$ cm s^{-1} and $(1.43\pm0.17)\times10^{-5}$ cm s^{-1} in normal and cancerous bladder tissues, respectively. The obtained results show a statistically significant difference in permeability of normal and cancerous tissue and indicate that the PC of 50% DMSO is about 1.13-and 1.21-fold higher than that of 30% glucose in normal bladder and cancerous bladder tissues, respectively. Thus, the quantitative measurements with the help of PCs from OCT images can be a potentially powerful method for bladder cancer detection.**

Keywords: *hyperosmotic agents, glucose, dimethyl sulfoxide, permeability, human normal and cancerous bladder tissues.*

1. Introduction

Urinary bladder carcinoma has been currently ranked the fifth most common cancer in the USA and the sixth in the developed world [1, 2]. A majority of cases of bladder cancer represent non-muscle invasive bladder cancer and the recurrence rates reported are as high as 75% in terms of cancer-specific survival [3, 4]. High recurrence rates lead to the necessity of subsequent close lifelong clinical follow-up with cytology as well as to repeated treatment in today's medical practice. The above-said makes bladder cancer one of the most expensive in terms of medical treatments [5]. Recent advancements in imaging techniques may improve bladder cancer detection and characterisation and enhance transurethral resection quality. Liu et al. [6] mainly assessed three clinically used imaging techniques, including fluorescence cystoscopy, narrow-band imaging and optical coherence tomography (OCT). Each imaging technique discussed has its advantages and disadvantages.

Improvement of diagnostic accuracy and resection thoroughness depends on visualisation and biopsy, which allow a clinician to assess the location and extent of the tumour. The motivation for new imaging technologies is aimed at improving the visualisation of tumours [7]. Fluorescence cystoscopy (FC) has been established as a standard method for early bladder cancer detection [8]. FC is particularly useful at improving the detection of flat lesions, such as carcinoma *in situ* (CIS) [9]. However, this technique has been related to a relatively high number of false-positive results, which is due to reactive changes and inflammations [10]. Narrow band imaging (NBI) uses narrow bandwidth radiation with centre wavelengths in the blue and green spectra to increase the contrast of mucosa and small vascular structures with a high resolution, without the use of intravesical instillations [11]. Geavlete et al. improved NBI cystoscopy, showing significant progress in tumour visual accuracy and detection [12]. Herr et al. [13] showed that the use of NBI was associated with fewer recurrences and longer recurrence-free intervals. The Clinical Research Office of the Endourological Society recently launched an international randomised trial to evaluate NBI [6]. As a result, NBI demonstrates better bladder cancer detection. In addition, further research is necessary to determine the long-term impact of two technologies on recurrence, progression and survival in the case of bladder cancer.

Pan et al. [14] demonstrated the utility of OCT in high-resolution imaging to delineate the micromorphology of highly scattering tissues such as urinary bladders; besides, they found OCT to be clinically relevant in diagnosing alternations or tumour growth in these tissues [14]. Imaging modality like OCT is a noninvasive optical imaging technique that has been developed for high-resolution *in vivo* examination and cross-sectional microstructure imaging of biological tissues or histological sections [15–21]. The layer thickness and attenuation coefficient of the OCT signal can be extracted from biological tissues in real-time [22–29]. The optical clearing technique can ensure deeper penetration of light into tissues by using optical clearing agents (OCAs) to reduce light scattering by tissue layers and blood, which improves image quality and precision of spectroscopic information from the tissue depth [30, 31].

In this paper, we have studied the permeability of glucose and dimethyl sulfoxide (DMSO) in normal and cancerous bladder tissues *in vitro* with OCT. The diffusion process of the agents in cancerous and normal bladder tissues was monitored with a spectral domain OCT (SD-OCT) during the

B. Lei, X. Deng, H. Wei, Z. Guo MOE Key Laboratory of Laser Life Science & Institute of Laser Life Science, College of Biophotonics, South China Normal University, Guangzhou 510631, Guangdong Province, China; e-mail: weihj@scnu.edu.cn;
G. Wu Department of Surgery, the First Affiliated Hospital, Sun Yat-Sen University, Guangzhou 510080, Guangdong Province, China;
H. Yang, S. Xie Key Laboratory of Optoelectronic Science and Technology for Medicine of Ministry of Education of China, Fujian Normal University, Fuzhou 350007, Fujian, China;
Y. He Graduate School at Shenzhen, Tsinghua University, Shenzhen 518055, Guangdong, China

Received 9 January 2014; revision received 24 March 2014
Kvantovaya Elektronika **44** (12) 1165–1169 (2014)
Submitted in English

experiment. This research may improve the capability of OCT utilised in cancer detection and help patients with bladder cancer tissues by providing prompt diagnosis.

2. Materials and methods

2.1. Materials

Patients volunteered for the research program conducted at the First Affiliated Hospital of Sun Yat-Sen University, China, signed consent forms, with the procedure being approved by the local Ethics Committee. Fresh surgical specimens of bladder tissues with thickness varying from 1.0 to 2.0 mm were excised in nine volunteers (five men and four women) aged 40 or older (average age of 48). All the bladder cancerous tissues were stored in a refrigerator at –70 °C until the measurement *in vitro*. During the experiment, bladder samples were grouped into two critical cases: normal bladder tissues and cancerous bladder tissues. Then, the samples with the lateral dimension of approximately 1.0×1.0 cm were prepared in a freezing state for measurements. Right before OCT experiments, samples were defrosted in physiological saline at room temperature for 30 min. Continuous imaging was performed for approximately 2 h and the room temperature was maintained at 20 °C throughout the experiment. The region of the samples was imaged for about 5 to 10 min before hyperosmotic agents were applied. Agents investigated in this experiment were 30% (w/v) glucose and 50% (v/v) DMSO. Continuous topical application of hyperosmotic agents and 2-D OCT functional imaging were performed from superficial tissues. No samples were used more than once.

2.2. OCT system

Measurements were performed by using a SD-OCT system (Figs 1 and 2). A low-coherence broadband superluminescent diode with centre wavelength of 830 nm, bandwidth of 40 nm and an output power of 5 mW was used as an optical source. The signal-to-noise ratio (SNR) of this SD-OCT system was measured to be 120 dB. The axial resolution was 12 μm and transverse resolution was 15 μm, determined by the focal spot size of the probe beam. The acquisition time per OCT image was about 180 ms, corresponding to an A-scan frequency of 2000 Hz and the frame rate of 20 fps. A computer was used to control the OCT system with a data acquisition software written in Labview 7.2-D. A single 2D OCT image was selected every one minute by scanning the incident beam over the sample surface in the lateral direction and in-depth (A-scan) scanning by the interferometer. Adjacent depth profiles could be displayed on a gray scale level in real time, resulting in an image comparable to histopathology, with resolutions up to 10 μm and at depths of around 2–3 mm. Altogether, more than 200 two-dimensional OCT images obtained in each experiment were stored in the personal computer for post-processing.

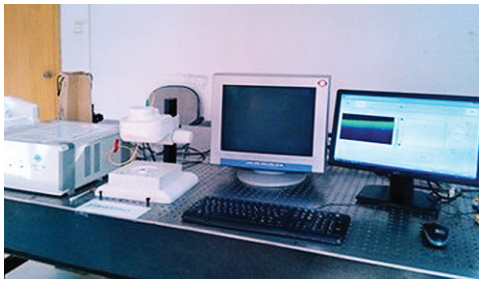

Figure 1. Experimental setup.

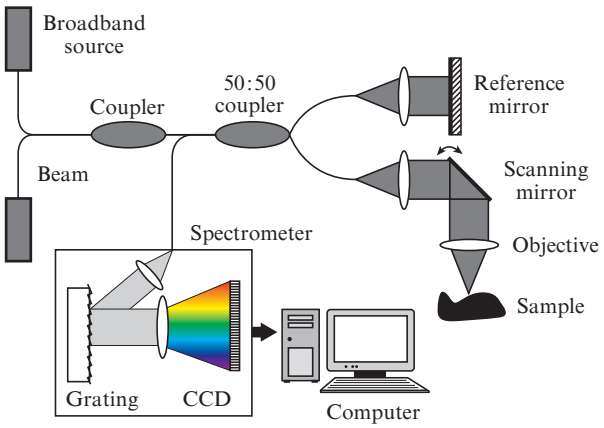

Figure 2. Schematic of the OCT system.

2.3. Methods

2D OCT images were obtained from the bladder tissues (both normal and cancerous) in each test and stored in a computer for further processing. The permeability coefficient (PC) of a hyperosmotic agent in a specific region of tissues *ex vivo* was calculated by analysing the slope changes in the OCT signal intensity during the diffusion process of the hyperosmotic agent in a specific depth region. This method was previously reported in detail in Refs [32–36].

In our work, the same method is applied to monitor and compute the differences in PCs of the glucose or DMSO diffusion in the normal human and bladder cancerous tissues. The 2-D OCT images were averaged in the lateral direction (x axis) (which is sufficient for speckle-noise suppression) into a single curve to obtain a 1-D OCT signal that represented a one-dimensional in-depth distribution of light. A region in the 1-D OCT signal intensity profile was chosen where the signal was relatively linear and underwent minimal alterations. Then, the slope was calculated from the chosen intensity profile for further analysis [37], with the calculated OCT signal slopes (OCTSS's) normalised and plotted as a function of time. The PCs of 30% (w/v) glucose and 50% (v/v) DMSO in normal and bladder cancerous tissue are calculated using the following equation: $P = z_{reg}/t_{reg}$, where z_{reg} is the thickness of the chosen section, and t_{reg} is the time for the glucose or the DMSO to diffuse through that section [38, 39]. The penetration time was measured from the point where the OCTSS's started to decrease to the point at which the reverse process began.

All the data from all the samples were presented as a 'mean ± standard deviation' and analysed by a paired-test. All statistical analyses were performed with the statistics software SPSS 10.0 for Windows.

3. Results and discussions

Figure 3 demonstrates a typical OCTSS graph for 30% (w/v) glucose diffusion experiments in human normal bladder tissue. The OCTSS of bladder tissue was calculated for the 80 μm region at a tissue depth of approximately 210 μm from the

tissue surface. Firstly, normal bladder tissue was monitored for about 8 min to record a baseline. Then, 0.1 mL of 30% glucose was topically applied to the OCT scanning area, where imaging continued for another 102 min. Diffusion of glucose solution inside bladder tissues dynamically changed the scattering coefficient, which was detected by OCT. The OCTSS decreased due to the reduction of scattering inside tissue caused by the local increase in glucose concentration. In Fig. 3, glucose solution reached the monitored region at approximately 12 min after application and took another 89 min to completely diffuse in the entire region. At that point, a reverse process in the OCTSS occurred. This reverse process is thought to stem from diffusion via concentration gradient differences on either side of tissue, which enforce the net fluid (mainly water) movement from the areas of higher concentration to the lower ones, thereby inducing water re-entry to the tissue after diffusion [40–43].

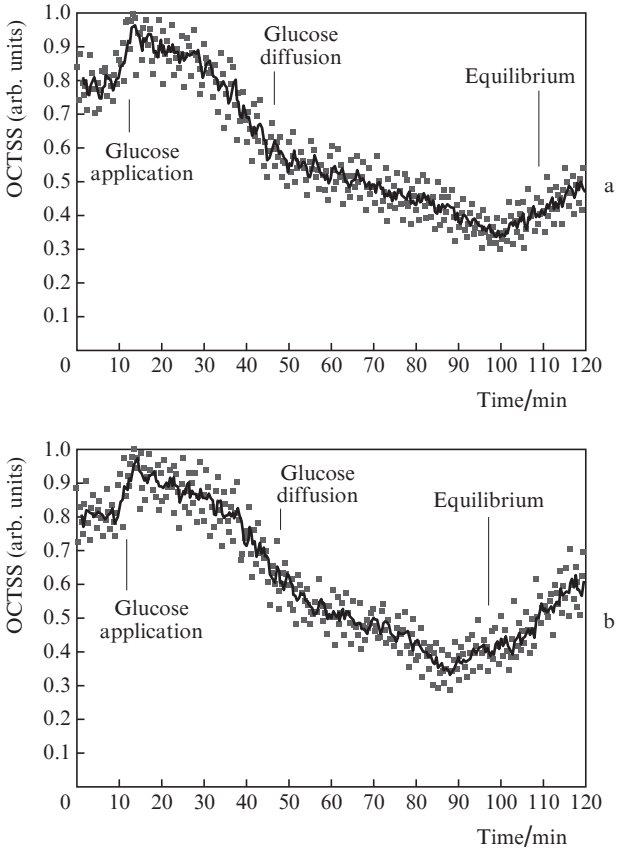

Figure 3. OCT signal slope as a function of time, recorded for (a) normal bladder tissue and (b) cancerous bladder tissue during 30% glucose diffusion; points show the experimental data.

Figure 3b shows a typical OCTSS graph for bladder cancerous tissue after application of 30% glucose. The trend of change in the OCTSS of bladder cancer tissue is similar to that of normal bladder tissue during 30% glucose diffusion experiments. The monitored regions are the same, but 30% glucose took about 14 min to reach the monitored region, and then only took about 67 min to completely diffuse.

Figure 3 shows that for each analyte, the dynamic OCTSS change trend of bladder cancerous tissues is similar to that of normal bladder tissues. However, the PCs of each analyte for these groups of tissues have a significant difference. This information could significantly increase the specificity and accuracy of tissue classification and the further use of OCT in clinical imaging.

With the same conditions and procedure, the OCTSS graphs of 50% (v/v) DMSO were obtained in diffusion experiments in normal and cancerous bladder tissues (Fig. 4).

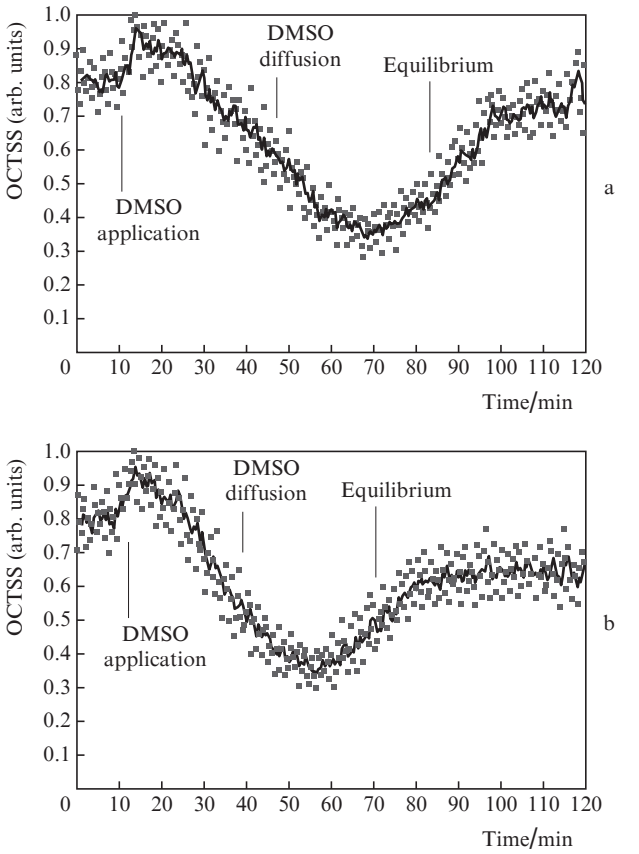

Figure 4. OCT signal slope as a function of time, recorded for (a) normal bladder tissue and (b) cancerous bladder tissue during 50% DMSO diffusion; points show the experimental data.

The average PCs of 30% glucose were estimated to be $(7.92 \pm 0.81) \times 10^{-6}$ cm s^{-1} and $(1.19 \pm 0.13) \times 10^{-5}$ cm s^{-1} in normal and cancerous bladder tissues, respectively, in ten independent experiments. The PCs of 50% DMSO were calculated to be $(8.99 \pm 0.93) \times 10^{-6}$ cm s^{-1} and $(1.43 \pm 0.17) \times 10^{-5}$ cm s^{-1} in normal and cancerous bladder tissues. The results with their corresponding standard deviation are shown in Fig. 5.

One of the most obvious characteristics is that the permeability in human bladder cancerous tissue is conspicuously higher than that in normal bladder tissue. For instance, the PC of 30% glucose increases by approximately 50.3% for cancerous tissue compared with that for normal bladder tissue, and the PC of 50% DMSO increases by approximately 59% for cancerous tissues compared with that for normal bladder tissue. This result well agrees with several previous studies that have been focused on the property of the permeability of hyperosmotic agents in normal and cancerous tissues [35, 40, 41, 44]. At the same time, our findings indicate that 50% DMSO has a higher PC compared to 30% glucose, no matter where it is used in normal or cancerous bladder tissues. The PC of 50% DMSO is about 1.13- and 1.21-fold higher than that of 30% glucose in normal and cancerous bladder tissues, respectively.

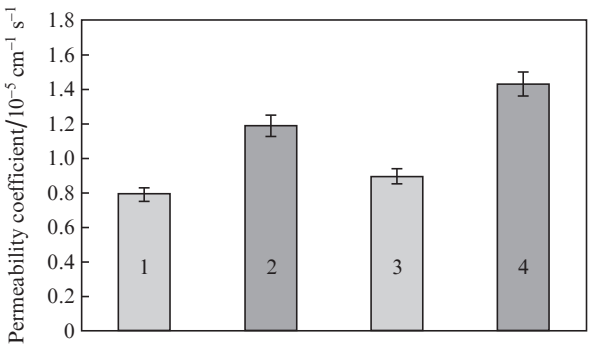

Figure 5. Average PCs of (1, 2) 30% glucose and (3, 4) 50% DMSO in (1, 3) normal and (2, 4) cancerous bladder tissues.

Recently, many studies analysed the relationship between tissue composition, microstructure and macrophysiology, showing that the bladder's physiological behaviour reflects both the mechanical properties of tissue and its complex structural organisation [4,21]. In particular, the difference can stem from the structure, composition of bladder tissues, structural properties of glucose and DMSO molecules.

Zhu et al. [45] made a conclusion that glucose is one of the most common analytes used as an optical clearing agent. It has been widely used to investigate the permeability of biological tissues. Compared with any other OCAs, glucose has many advantages, because its molecules are physiologically important and have excellent biocompatibility as an inert chemical compound. Glucose enters most cells by facilitating diffusion (moving down the concentration gradient across the cell membrane with help of a carrier protein). Nevertheless, diffusion of glucose in bladder tissues has never been studied. In previous studies, the average PCs have been reported in 30% glucose solution in human normal and cancerous lung tissues, colon tissues *in vitro* [46,47]. Comparison of the results of the current study with previous studies shows a significant increase in the PC of 30% glucose in normal and cancerous bladder compared with that of 30% glucose in lung and colon tissues, respectively, i.e., the optical clearing effects of 30% glucose *in vitro* in normal and cancerous human bladder are significantly different compared to other human tissues.

DMSO is a dipolar aprotic solvent, which has a tendency to accept rather than donate protons. Anhydrous DMSO has a refractive index of about 1.48. McClure et al. [48] demonstrated that DMSO is the only individual agent which possesses an appreciable optical clearing potential (a three-fold reduction in reduced optical scattering, according to our recent data on topical application). DMSO is medically approved in the USA only for the treatment of interstitial cystitis, a type of inflammation of bladder [49]. Although, DMSO currently is a shunned chemical agent due to its purported systemic toxicity, the FDA ultimately concluded that clinical studies of DMSO are still warranted to demonstrate both the efficacy and safety of DMSO based on data from Ref. [49]. Assessment of the effects of 50% DMSO on permeability of normal and cancerous human bladder tissues with a SD-OCT system shows that DMSO resulted in a marked increase in the PC.

4. Conclusions

In this paper, we have measured the optical permeability coefficients of glucose and DMSO in normal and cancerous bladder tissue groups using SD-OCT and analysed the changes of the PCs in the region of interest. The results obtained indicate that the cancerous bladder tissue has a higher optical PC than that in normal bladder tissue. As to the optical clearing efficacy, the PC of 50% DMSO is about 1.13- and 1.21-fold higher than that of 30% glucose in normal and cancerous bladder tissues, respectively. These findings support the hypothesis that OCT can be used to measure the PC, and show a statistically significant difference in permeability of normal and cancerous tissue ($p < 0.05$). These results suggest that quantitative analysis of bladder tissue optical properties by SD-OCT could be used for differentiation of cancerous human bladder tissue from normal tissue and early diagnosis of bladder cancerous tissue. Our future work will focus on investigating the effect of topical application of OCAs on bladder tissues *in vivo* and choosing the optimal concentration of hyperosmotic chemical agents according to different stages of bladder cancer.

Acknowledgements. This work was supported by the National Natural Science Foundation of China (Grant Nos 61335011, 61275187, 81071790 and 81171379), Specialized Research Fund for the Doctoral Program of Higher Education of China (Grant Nos 20114407110001 and 200805740003), the Science and Technology Innovation Project of the Education Department of Guangdong Province of China, the Natural Science Foundation of Guangdong Province of China (Grant No. 9251063101000009) and Key Laboratory of Optoelectronic Science and Technology for Medicine (Fujian Normal University), Ministry of Education, China (Grant No. JYG1202).

References

1. Jemal A., Siegel R., Xu J., Ward E. *Ca-Cancer J. Clin.*, **60**, 277 (2010).
2. Jemal A., Bray F., Center M.M., Ferlay J., Ward E., Forman D. *Ca-Cancer J. Clin.*, **61**, 69 (2011).
3. Dindyal S., Nitkunan T., Bunce C.J. *Photodiag. Photodyn. Ther.*, **5**, 153 (2008).
4. Sylvester R.J., van der Meijden A.P., Oosterlinck W., Witjes J.A., Bouffioux C., Denis L., Newling D.W., Kurth K. *Eur. Urol.*, **49**, 466 (2006).
5. Botteman M.F., Pashos C.L., Redaelli A., Laskin B., Hauser R. *Pharmacoeconomics*, **21**, 1315 (2003).
6. Liu J.J., Droller M.J., Liao J.C. *J. Urol.*, **188**, 361 (2012).
7. Evelyne C.C., De La Rosette J.J., De Reijke T.M. *Indian J. Urol.*, **27**, 245 (2011).
8. Witjes J.A., Douglass J. *Nat. Clin. Pract. Urol.*, **4**, 542 (2007).
9. Jichlinski P., Guillou L., Karlsen S.J., Malmström P.U., Jocham D., Brennhovd B., Johansson E., Gärtner T., Lange N., Van den Bergh H., Leisinger H.J. *J. Urol*, **170**, 226 (2003).
10. Lovisa B., Jichlinski P., Aymon D., Van Den Bergh H., Wagnières G. *Proc. SPIE Int. Soc. Opt. Eng.*, **6842**, 684218 (2008).
11. Cauberg E.C., Kloen S., Visser M., de la Rosette J.J., Babjuk M., Soukup V., Pesl M., Duskova J., De Reijke T.M. *Urology*, **76**, 658 (2010).
12. Geavlete B., Jecu M., Multescu R., Geavlete P. *Ther. Adv. Urol.*, **4**, 211 (2012).
13. Herr H.W., Donat S.M. *BJU Int.*, **107**, 396 (2011).
14. Pan Y., Lavelle J., Bastaky S., Farkas D.L., Zeidel M.L. *Proc. SPIE Int. Soc. Opt. Eng.*, **4224**, 391 (2000).
15. Drexler W.J. *Biomed. Opt.*, **9**, 47 (2004).
16. Siegel R., Naishadham D., Jemal A. *Ca-Cancer J. Clin.*, **62**, 10 (2012).
17. Gladkova N., Streltsova O., Zagaynova E., Kiseleva E., Gelikonov V., Gelikonov G., Karabut M., Yunusova K., Evdokimova O. *J. Biophotonics*, **4**, 519 (2011).
18. Bouma B.E., Tearney G.J., Compton C.C., Nishioka N.S. *Gastrointest. Endosc.*, **51**, 467 (2000).

19. Fujimoto J.G., Pitris C., Boppart S.A., Brezinski M.E. *Neoplasia*, **2**, 9 (2000).
20. Cauberg E.C., De Bruin D.M., Faber D.J., Van Leeuwen T.G., De la Rosette J.J., De Reijke T.M. *Eur.Urol.*, **56**, 287 (2009).
21. Cauberg E.C., De Bruin D.M., Faber D.J., De Reijke T.M., Visser M., De La Rosette J.J., Van Leeuwen T.G. *J. Biomed. Opt.*, **15**, 066013 (2010).
22. Patel P., Bryan R.T., Wallace D.M.A. *The Scientific World J.*, **11**, 2550 (2011).
23. Sengottayan V.K., Vasudeva P., Dalela D. *Indian J. Urol.*, **24**, 592 (2008).
24. Osiac E., Săftoiu A., Gheonea D.I., Mandrila I., Angelescu R. *World J. Gastroentero*, **17**, 15 (2011).
25. Goh A.C., Lerner S.P. *World J. Urol.*, **27**, 301 (2009).
26. Ascencio M., Collinet P., Cosson M., Mordon S.J. *Gynecol. Obstet. Biol. Reprod*, **36**, 749 (2007).
27. Ikeda M., Matsumoto K., Choi D., Nishi M., Fujita T., Ohbayashi K., Shimizu K., Iwamura M. *BMC Urol.*, **13**, 65 (2013).
28. Schmidbauer J., Remzi M., Klatte T., Waldert M., Mauermann J., Susani M., Marberger M. *Eur.Urol.*, **56**, 914 (2009).
29. Lerner S.P., Goh A.C., Tresser N.J., Shen S.S. *Urology*, **72**, 133 (2008).
30. Larina I.V., Carbajal E.F., Tuchin V.V., Dickinson M.E., Larin K.V. *Laser Phys. Lett.*, **5**, 476 (2008).
31. Tuchin V.V., Tuchin V. *Tissue Optics: Light Scattering Methods and Instruments for Medical Diagnosis* (Bellingham: SPIE Press, 2007) Vol. TT13.
32. Tuchin V.V. *J. Phys. D: Appl. Phys.*, **38**, 2497 (2005).
33. Larin K.V., Motamedi M., Ashitkov T.V., Esenaliev R.O. *Phys. Med. Biol.*, **48**, 1371 (2003).
34. Esenaliev R.O., Larin K.V., Larina I.V., Motamedi M. *Opt. Lett.*, **26**, 992 (2001).
35. Ghosn M.G., Carbajal E.F., Befrui N.A., Tuchin V.V., Larin K.V. *J. Biomed. Opt.*, **13**, 021110 (2008).
36. Yeh A.T., Hirshburg J. *J. Biomed. Opt.*, **11**, 014003 (2006).
37. Ghosn M.G., Sudheendran N., Wendt M., Glasser A., Tuchin V.V., Larin K.V. *J. Biophoton.*, **3**, 25 (2010).
38. Larin K.V., Ghosn M.G., Ivers S.N., Tellez A., Granada J.F. *Laser Phys. Lett.*, **4**, 312 (2007).
39. Ghosn M.G., Tuchin V.V., Larin K.V. *Invest. Ophthalmol. Vis. Sci.*, **48**, 2726 (2007).
40. Zhong H.Q., Guo Z.Y., Wei H.J., Zeng C.C., Xiong H.L., He Y.H., Liu S.H. *Laser Phys. Lett.*, **7**, 315 (2010).
41. He Y.H., Wang R.K. *J. Biomed. Opt.*, **9**, 200 (2004).
42. Zhao Q.L., Si J.L., Guo Z.Y., Wei H.J., Yang H.Q., Wu G.Y., Xie S.S., Li X.Y., Guo X., Zhong H.Q., Li L.Q. *Laser Phys. Lett.*, **8**, 71 (2011).
43. Xiong H.L., Guo Z.Y., Zeng C.C., Wang L., He Y.H., Liu S.H. *J. Biomed. Opt.*, **14**, 024029 (2009).
44. Ghosn M.G., Carbajal E.F., Befrui N.A., Tellez A., Granada J.F., Larin K.V. *J. Biomed. Opt.*, **13**, 010505 (2008).
45. Zhu Z., Wu G., Wei H., Yang H., He Y., Xie S., Zhao Q., Guo X. *J. Biophoton.*, **5**, 536 (2012).
46. Zhao Q., Zhou C., Wei H., He Y., Chai X., Ren Q. *J. Biomed. Opt.*, **17**, 1050041 (2012).
47. Chen D., Song D., Wientjes M.G., Au J.L. *Clin. Cancer Res.*, **9**, 363 (2003).
48. McClure R.A., Stoianovici C., Karma S., Choi B. *Proc. SPIE Int. Soc. Opt. Eng.*, **7187**, 718707 (2009).
49. Bui A.K., McClure R.A., Chang J., Stoianovici C., Hirshburg J., Yeh A.T., Choi B. *Laser Surg. Med.*, **41**, 142 (2009).